Journal of Petroleum Research and Studies

Open Access
No. 34 part 1, March 2022, pp. 85-104

P- ISSN: 2220-5381
E- ISSN: 2710-1096

DOI: http://doi.org/10.52716/jprs.v12i1.592

Simulation of a Perforated Vertical Wellbore with Near Wall Porous Media Effect

Haider S. Mohammed[1,*], Hussein S. Sultan[2], Emad A. Khazal[3]
Department of Petroleum Engineering, College of engineering, University of Basra, Basra City, Iraq,
[1,*]Corresponding Author E-mail: Lec.haider.sami@uobasrah.edu.iq
[2]Hussein.sultan@uobasrah.edu.iq,[3]Emad.ab74@gmail.com

6th Iraq Oil and Gas Conference, 29-30/11/2021

Abstract

This paper aims to predict the effect of porous media permeability and perforations parameters on the pressure drop and productivity index, for the perforated vertical wellbore with six perforations and for two phase angles. The first 60° phase angle with helical distribution and the second 180° phase angle with normal distribution. In this study, a Computational Fluid Dynamics (CFD) software has been used to simulate a model of 3-D turbulent fluid flow with stander k−∈, steady-state, and single phase. The effect of the permeability of porous media, inlet mass flow rate from porous media, perforations length, and diameter of perforations are studied, for two cases of the phase angles. The results of this study show that, the pressure drop decreases with increasing permeability pf porous media, so the productivity index increasing. Also, increase of inlet mass flow rate from porous media causing an increase in the pressure drop. The perforations length has a few effects on the pressure drop and productivity index, while the diameter of perforations has a greater effect on the pressure drop.

Keywords: wellbore, perforation, permeability, porous media, Computational Fluid Dynamics.

الخلاصة

يهدف هذا البحث إلى التنبؤ بتأثير نفاذية الوسائط المسامية وتاثير الثقوب على انخفاض الضغط ومؤشر الإنتاجية ، لحفرة البئر العمودية المثقبة، تحتوي على ستة ثقوب ولزوايا طور مختلة. الزاوية الأولى 60 درجة مع التوزيع الحلزوني وزاوية الطور الثانية 180 درجة مع التوزيع الطبيعي. في هذه الدراسة، تم استخدام برنامج ديناميكيات الموائع الحسابية (CFD) لمحاكاة نموذج لتدفق السوائل المضطرب ثلاثي الأبعاد مع معيار k −∈، والحالة المستقرة، وطور واحد. تمت دراسة تأثير نفاذية الوسائط المسامية ومعدل تدفق كتلة المدخل من الوسط المسامي ،وطول الثقوب، وقطر الثقوب لحالتين من زوايا الطور. أظهرت نتائج هذه الدراسة أن انخفاض الضغط يتناقص مع زيادة نفاذية الوسائط المسامية، وبالتالي يزداد مؤشر الإنتاجية. أيضا، زيادة

Open Access
No. 34 part 1, March 2022, pp. 85-104
P- ISSN: 2220-5381
E- ISSN: 2710-1096

معدل تدفق كتلة المدخل من الوسائط المسامية مما يؤدي إلى زيادة انخفاض الضغط. طول الثقوب له تأثيرات قليلة على انخفاض الضغط ومؤشر الإنتاجية، بينما يكون لقطر الثقوب تأثير أكبر على انخفاض الضغط.

1. Introduction

The formation damage is a serious problem in oil and gas industry. The formation damage caused by drilling-fluid invasion, production, or injection can leads to positive skin factors and affect fluid flow by reducing the permeability of the formation surrounding a wellbore. Many researchers focused on their study on the effects of perforation parameters and permeability zone surrounding the wellbore. The effect of perforation parameters on the main inflow efficiency are studied using analytical calculations derived by Muskat [1]. He analytical calculations to determine the effect of spacing between perforations and shot density on productivity of perforated vertical wells. He determined that the well productivity can be identified by the shot density and the distribution of perforations. Locke [2] presented a new theoretical method to predict the productivity ratio of a perforated vertical wellbore by constructing a more accurate simulation model, a finer finite element method was used to run simulations. He focused on the effect of perforation length, perforation phase angle, perforation diameter, shot density, crushed zone effect and damaged zone effect on productivity ratio. Deo et al. [3] studied two types of flow targets; linear target (unperforated) and radial target (perforated) in a cylindrical laboratory sample to determine which of these targets best represents downhole conditions, using a 3D finite element to calculate inflow into perforations. The effects of shot density and perforation phase angle were investigated by them. Their results showed that neither linear nor radial targets provided a perfect model for inflow from perforations. Karakas and Tariq [4] presented a semi-analytical solution to predict the productivity ratio of perforated vertical wellbore, using 2D and 3D finite element for flowrate performance of the perforations. Their results showed that the productivity ratio increases with increasing perforation length and the crushed zone around perforations essentially increases the vertical resistance to flow. Ihara et al. [5] presented an experimental study for single phase flow in a channel of rectangular cross-section with inflow through porous walls to predict the pressure drop in a horizontal wellbore. The frictional pressure drop in the model was treated as that for flow in a pipe. Dogulu [6] presented a numerical model to estimate the productivity of perforated

Open Access
No. 34 part 1, March 2022, pp. 85-104
P- ISSN: 2220-5381
E- ISSN: 2710-1096

horizontal, vertical and slanted wells as a function of shot density, perforations length, and phasing angles. He used FDM for a single phase and algebraic grid generation technique to build the grid of perforated wellbore. Tang et al. [7] presented a comprehensive study on a horizontal well with slotted-liners or perforation completion to obtain the productivity ratio, based on semi analytical model that couples a reservoir and wellbore fluid flow equations. they showed that both perforation length and density has a significant effect on productivity. Ansah et al. [8] presented a new 3D model for a vertical wellbore to predict the effect of the perforations length, casing (pipe) diameter, perforations density, perforations phase angles, and the degree of damage inside and around the perforations on the productivity ratio and skin factor, using a 3D finite element model ANSYS 5.7 to obtain a result to demonstrate the improvements of the flow rate predictions. Guerra and Yildiz [9] presented a simple approximate model to predict the inflow performance of perforated vertical wellbore, using a programmable calculator to solve algebraic equations and compared with analytical solution of SPAN software. Yildiz [10] reviewed the methods used to predict the productivity ratio and total skin factor of perforated vertical, horizontal and inclined wellbore, and compared the results with experimental analysis. The results showed that the productivity ratio increases and the total skin factor decrease with increasing perforation length. Hagoort [11] presented an analytical model to predict the productivity ratio of a perforated vertical wellbore, based on the analytical solution for a single phase Darcy flow for a single perforation with considered the effect of perforation damage. Kuljabekov et al. [12] presented a numerical solution for the technology of multistage filters setting in porous media near a vertical wellbore. Using Darcy and conservation laws to describe the fluid flow in a homogeneous and isotropic medium. Elsharafi et al. [13] explained how to evaluate the different perforation parameters of the production vertical oil wells by using well test reservoir description and perforation information. The necessary data have been collected from Hungarian oil wells including reservoir description data from the MOL Company files. This study was concentrated on the effects of damaged skin factor, crushed zone skin factor and perforation skin factor. Also, calculation method for the perforation depth and flow rate for different kinds of the gun are used.

Open Access
No. 34 part 1, March 2022, pp. 85-104
P- ISSN: 2220-5381
E- ISSN: 2710-1096

The aims of this study is to assess the effect of porous zone permeability surrounding vertical wellbore and inlet mass flow rate from porous media on the pressure drop, productivity index, pressure and velocity distribution surrounding the wellbore. Also, the effect of diameter and length of perforations are studied. Also, the comparison between normal and helical distribution for the perforations will be viewed.

2. Description of the Cases

In this work, the effect of porous media surrounded the wellbore and the parameters of perforation on the pressure drop and productivity index are studied. The simulation performed for two models as shown in Figure (1). The first was normal distribution with 180^{o} phase angle, and the second was the helical distribution of perforations with 60^{o} phase angle, for six conical-shaped perforations. The vertical wellbore of (D=0.1524 m) in diameter and of (L=1 m) in length through axial centerline along the Y-axis, with perforations perpendicular on the vertical wellbore. Where diameter (d_1= 13mm) cutting the vertical wellbore at entrance and diminish to the diameter (d_2=8 mm) through the length (l_p=0.3 m). The space vertical between each two successive perforations is (h) 0.1 m. The diameter of the area surrounding the wellbore (D_p) is 3 m with permeability (k=100 md) and porosity is (ϕ=0.35) as shown in Figure (2).

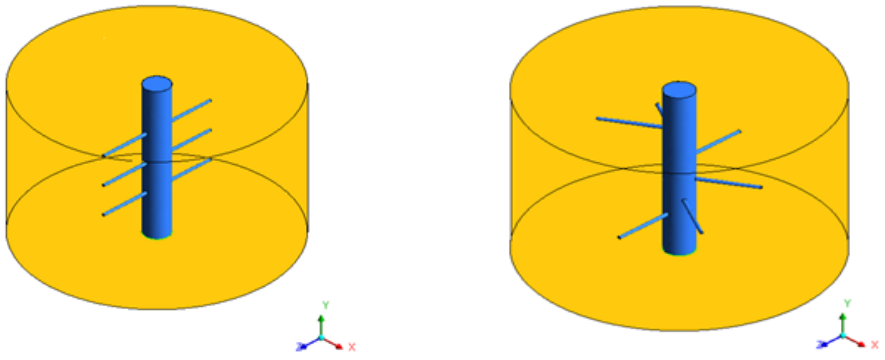

(a)3D model for 180^{o} phase angle with with Normal distribution.

(b)3D model for 60^{o} phase angle with Helical distribution.

Fig. (1): The geometry of a perforated vertical wellbore with different perforation phase angles.

Open Access
No. 34 part 1, March 2022, pp. 85-104
P- ISSN: 2220-5381
E- ISSN: 2710-1096

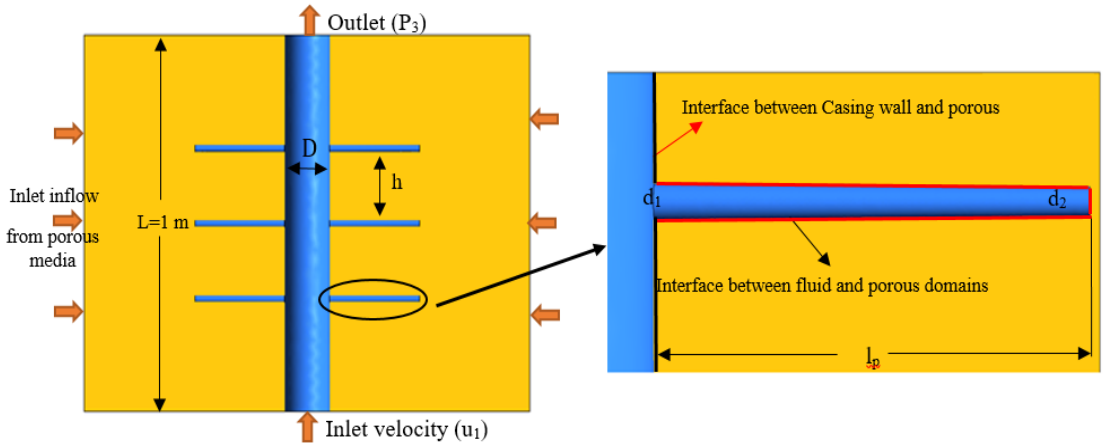

Fig. (2): Vertical wellbore with porous media for 6 perforations with 180° phase angle with normal distribution.

3. Governing Equations

The fluid flow and heat loss in the perforated vertical wellbore with the porous media undergoes a considerable measure of physical changes such as pressure drop due to friction losses in the vertical pipe and perforations, mixing, acceleration and gravity, velocity change caused by varying inflow regimes and density, and kinetic energy change. In order to properly describe these physical changes, we need two governing equations of the fluid inflow (mass and momentum equations) [14, 15, and 16].

Conservation of Mass: The mass conservation equation describes the fluid inflow velocity and density change along the wellbore. It is expressed by the equation below:

$$\rho \frac{\partial}{\partial x_i}(u_i) = 0 \qquad (1)$$

Conservation of Momentum: The momentum conservation equations in the Cartesian coordinate are given below:

$$\frac{\partial}{\partial t}(\rho u_i) + u_j \frac{\partial(\rho u_i)}{\partial x_j} = -\frac{\partial P}{\partial x_i} + \frac{\partial}{\partial x_j}(\tau_{ji}) + F_i \qquad (2)$$

The Forchheimer's equation is used to describe the flow through the porous media at perforation and expressed mathematically as follows [17];

$$-\nabla P = \left(\frac{\mu}{k}\right) \mathrm{u}_i + \beta\rho|\mathrm{u}|\mathrm{u}_i \qquad (3)$$

Open Access
No. 34 part 1, March 2022, pp. 85-104
P- ISSN: 2220-5381
E- ISSN: 2710-1096

where ∇P is the pressure gradient, *k* is the permeability of porous media, μ is a fluid viscosity, u_i is the Forchheimer coefficient and u_i is the Darcy/Forchheimer velocity.

4. CFD Model Solution Method

Simulation of fluid flow using CFD involves the following five steps: creating the computational model (2D or 3D geometry); surface or volume meshing; preprocessing (definition of fluid domains, physical models, and boundary and initial conditions); numerical solution; and post-processing of simulation results. The assumptions are (single phase, Newtonian flow, turbulent flow and isothermal conditions), and k-ε model used for turbulent flow. The properties of the crude oil are (density is 842 kg/m3 and viscosity is 0.006kg/m.s) at temperature 65 °C.

4.1 Boundary Condition

(i) The inlet velocity of the wellbore (u_1) is 1.5 m/s and the inlet velocity from porous media is 0.5 kg/s.

(ii) The pressure (P_3) at exit of the wellbore is equal to zero. As shown in Figure (2).

(iii) The roughness of the casing wall is equal to 0.02 mm.

(iv) No slip velocity at the walls.

(v) Constant temperature (isothermal) of 65 °C.

5. CFD model validation

In order to verify the accuracy of the CFD model. A comparison with the results of [18] is performed. The flow geometry is a 3D vertical pipe with two perforations at middle and the diameter of the perforations are 0.012 m; length is 0.15 m and 180° the perforations phase angle. The diameter of the pipe is 0.2 m and the length is 1 m. The boundary conditions of this validation are as follow; inlet mean velocity (u1= 2.5 m/s), inlet velocity from perforations (u2=1 m/s), while the static pressure at the outlet equal to zero. Figure (3) shown the results of this validation for the static pressure drop along the centerline of the pipe, the results show a good agreement with the work of Salim et al., and the percentage error between Salim et al. and present work is less than 1.6%.

Open Access
No. 34 part 1, March 2022, pp. 85-104
P- ISSN: 2220-5381
E- ISSN: 2710-1096

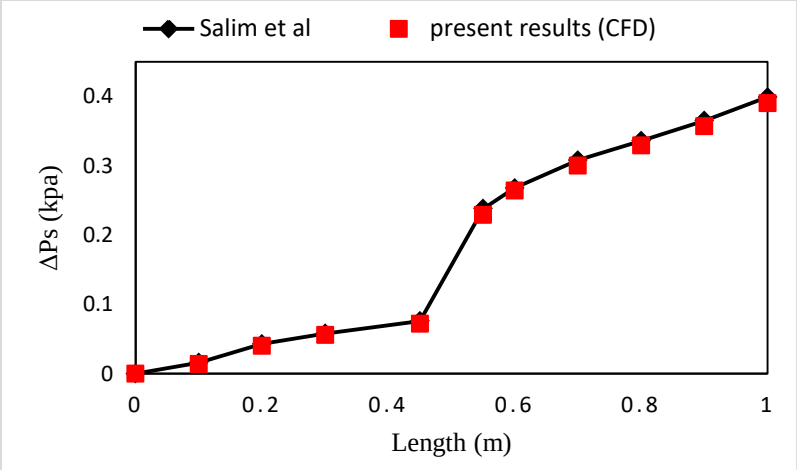

Fig. (3): Comparison between the present work and the data of [18]

5. Results and Discussion

The effect of the porous media surrounding the wellbore and perforation parameters was studied. The numerical simulation for a perforated vertical wellbore with 6 conical shape perforations and two phase angle was performed. The first was 60° phase angle with helical distribution and the second was 180° phase angle with normal distribution. The perforation diameters are (d1=13 mm, d2=8 mm) and length is (0.3 m) with the vertical space between two successive perforations is 0.1 m. The vertical wellbore of (0.1524 m) in diameter and of (1 m) in length and surrounded by a porous media of diameter (1.5 m) and height (1 m), the permeability of porous media is (1×10^{-13} m^2) and porosity is (0.35).

5.1 Effect of the porous media surrounding wellbore

Figure (4) shows the variation of the pressure drop in the wellbore with porous media permeability, for two cases of the phase angles. The pressure drop decreases with increasing permeability of porous media for the two cases, due to the decrease of pressure at the boundaries of the porous media, this leads to reduces the inflow of fluid from perforations to the wellbore. Also, the pressure drop for 180° phase angle with normal distribution is greater than 60° phase angle with helical distribution. This difference is due to that the obstacle for the fluid inflow for 180° phase angle with normal distribution is great than of 60° phase angle with helical distribution as shown in Figure (5).

Open Access
No. 34 part 1, March 2022, pp. 85-104
P- ISSN: 2220-5381
E- ISSN: 2710-1096

Figure (6) illustrates the variation of the productivity index with different permeability of the porous media. The productivity index increases with increased permeability of the porous media, due to a decrease in the pressure drop of the wellbore.

Figure (7) shows the contours of pressure distribution for different porous media surrounding the wellbore for two cases of the phase angle. The first 60° phase angle with helical distribution and the other 180° phase angle with normal distribution. The pressure distribution contour shows that, the maximum pressure at the boundary of the porous media surrounding the wellbore. The values of maximum pressure decreases with increasing permeability, due to decreasing fluid flow resistance. Also, figure (8) shows the pressure contour for porous media surrounding the wellbore in a horizontal plane with the middle of the wellbore.

Figure (9) shows the velocity contour for a perforated vertical wellbore with surrounding porous media, for inlet velocity of the wellbore is 1.5 m/s, inlet mass flow rate from porous media is 0.5 kg/s and the outlet pressure is equal to zero. From the figure, the maximum velocity in the case 60° helical distributions is greater than 180° normal distributions, due to obstruction of fluid flow in the wellbore for the 180˚ phase angle greater than 60˚ phase angle.

Figure (10) presents the velocity streamlines for a perforated vertical wellbore with surrounding porous media. It can be inferred that radial flow occurs away from the wellbore, and then flow becomes 3D as fluid approaches the perforation tunnels.

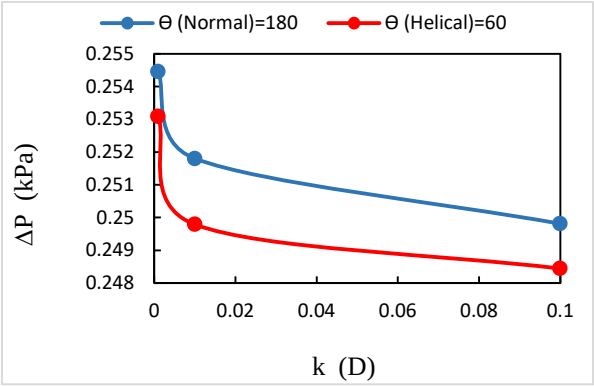

Fig. (4): Variation of the pressure drop with different permeability of porous media.

Open Access
No. 34 part 1, March 2022, pp. 85-104
P- ISSN: 2220-5381
E- ISSN: 2710-1096

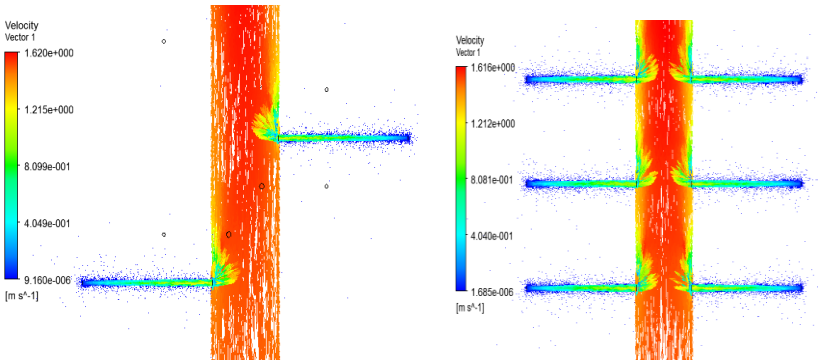

(a) 60° phase angle (b)180° phase angle

Fig. (5): Velocity vector for 6 perforations of vertical wellbore with k=0.1 D

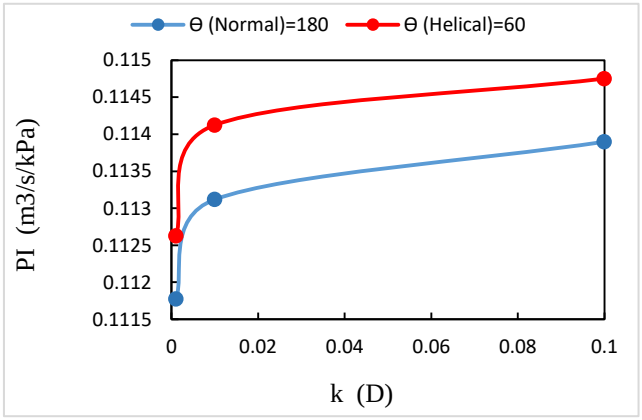

Fig. (6): Variation of productivity index with different permeability of porous media.

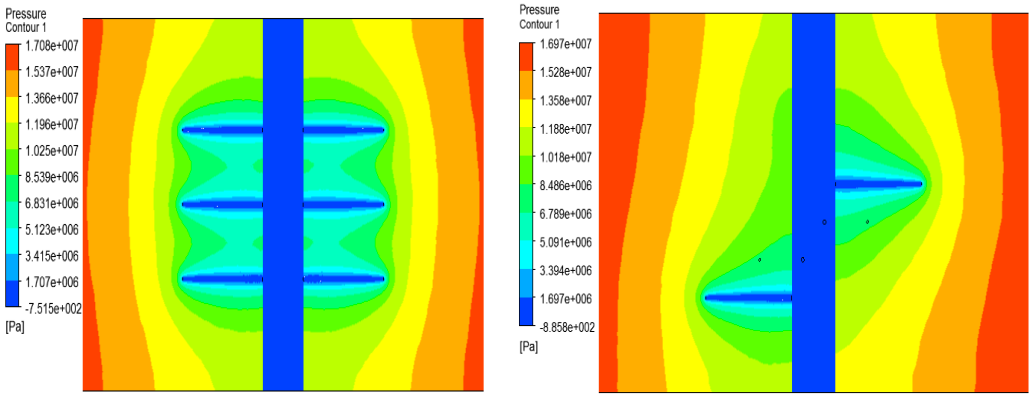

(a)180° phase angle with k=0.1 D (b) 60° phase angle with k=0.1 D

Fig. (7): Pressure distributions contour with different of phase angles and porous media permeability.

Open Access
No. 34 part 1, March 2022, pp. 85-104
P- ISSN: 2220-5381
E- ISSN: 2710-1096

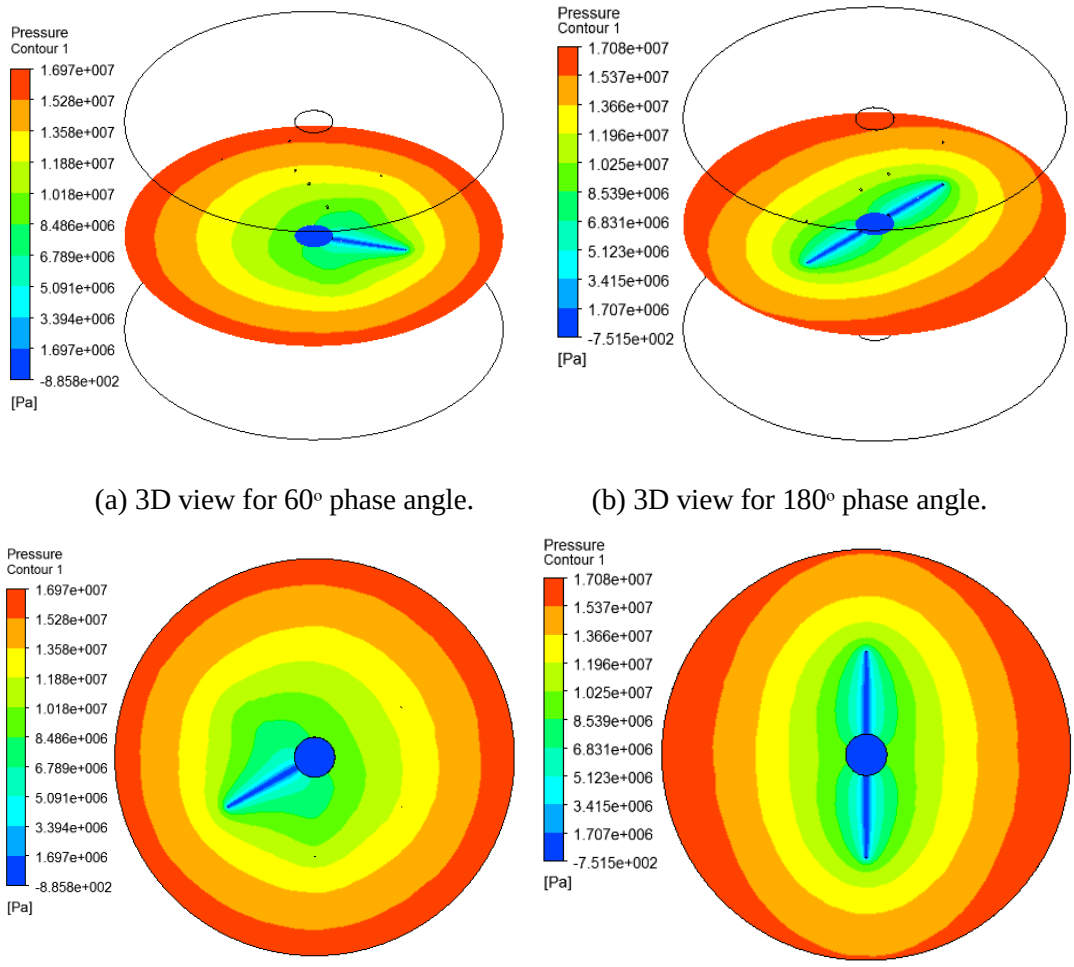

(a) 3D view for 60° phase angle. (b) 3D view for 180° phase angle.

(c) 2D view for 60° phase angle. (d) 2D view for 180° phase angle.

Fig. (8): The contours of pressure distribution surrounding of the wellbore with k=0.1 D

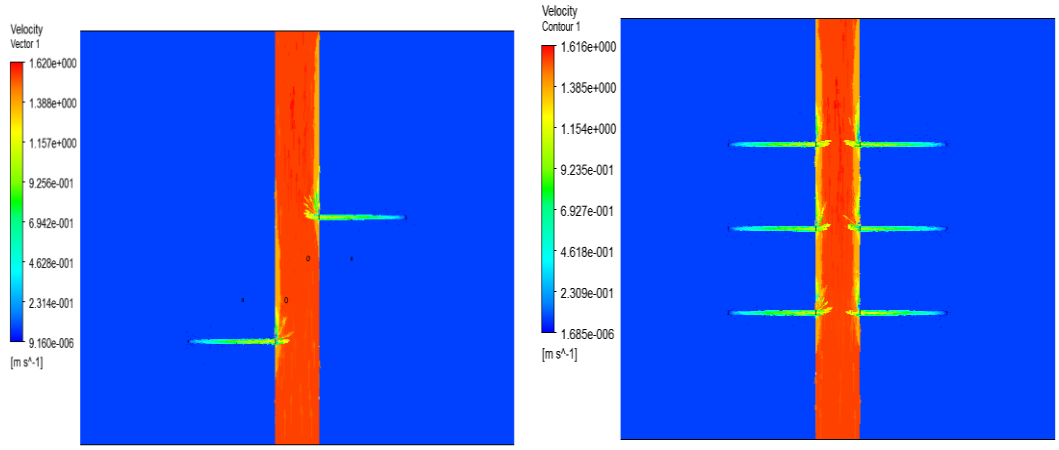

(a) 60° phase angle (b) 180° phase angle

Fig. (9): The velocity contours for 6 perforations with k=0.1 D.

Open Access
No. 34 part 1, March 2022, pp. 85-104
P- ISSN: 2220-5381
E- ISSN: 2710-1096

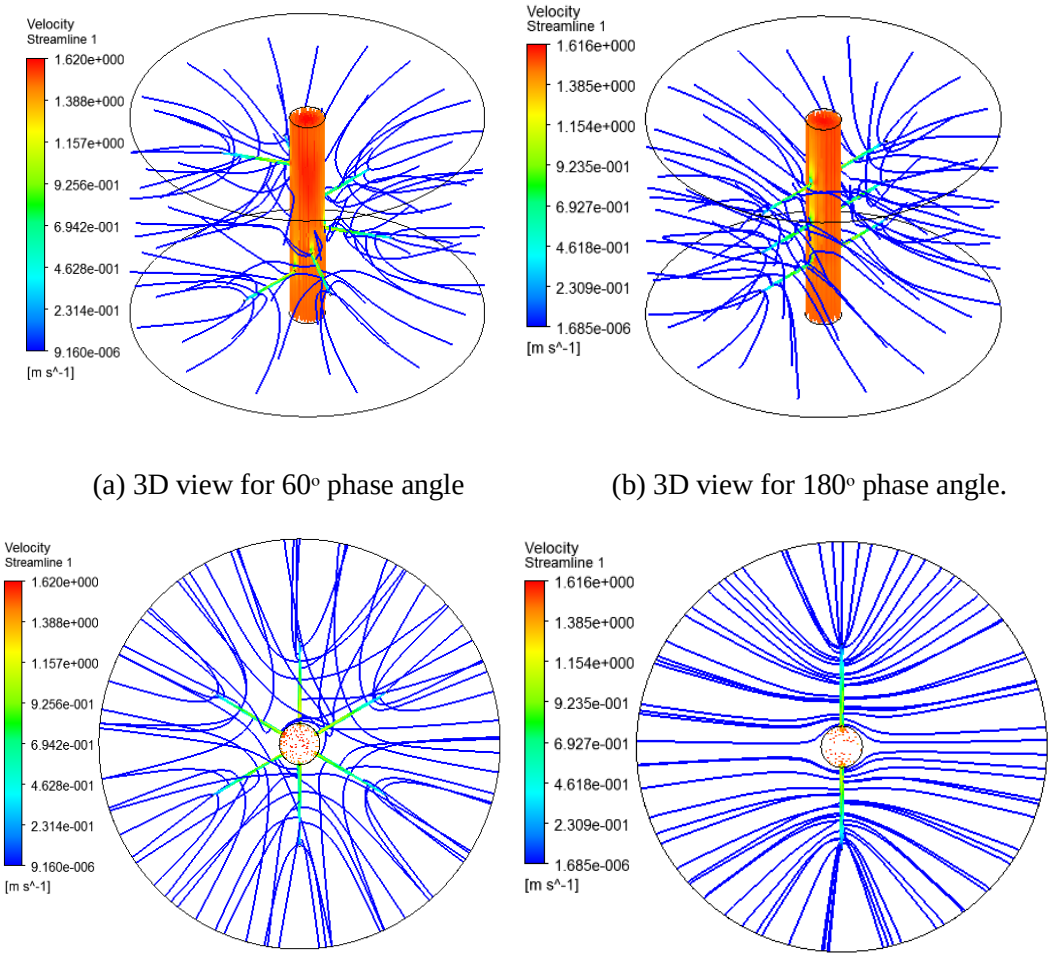

(a) 3D view for 60° phase angle

(b) 3D view for 180° phase angle.

(c) 2D view for 60° phase angle.

(d) 2D view for 180° phase angle.

Fig. (10): The velocity streamline for 6 perforations of vertical wellbore with k=0.1 D.

The pressure drop and productivity index in a perforated vertical wellbore is affected by inlet mass flow from the porous media. Figure (11) demonstrate the variation of the pressure drop with inlet mass flow rate from porous media, for four values of the inlet mass flow rate from porous media which are (0.4, 0.5, 0.6, 0.7 kg/s). The pressure drop increases with increasing inlet mass flow rate from porous media, due to an increase of fluid inflow rate from perforations to the wellbore.

Figure (12) illustrates the variation of the productivity index with inlet mass flow rate from porous media surrounding the wellbore for two phase angles, 60° phase angle with helical distribution and 180° phase angle with normal distribution. The productivity index decreases with increasing inlet mass flow rate from porous media, due to an increase of the pressure drop in the wellbore.

Open Access
No. 34 part 1, March 2022, pp. 85-104
P- ISSN: 2220-5381
E- ISSN: 2710-1096

Figure (13) demonstrate the pressure contours for the near-wellbore region with different values of the inlet mass flow rate from the porous media, for 60° phase angle with helical distribution and 180° phase angle with normal distribution. The pressure contours show that, the maximum pressure at the external boundaries, and then the pressure begins to decrease when approaching the wellbore due to the resistance of the fluid flow. Also, the increase of the mass flow rate required high pressure at the porous media surrounding the wellbore.

Figure (14) shows the velocity contour for the perforated vertical wellbore with the surrounding porous media. For the inlet velocity of wellbore is 1.5 m/s, the inlet velocity from porous media is 0.5 kg/s and the outlet pressure is equal to zero. The highest fluid velocity occurs inside the perforation. Also, the velocity maximum for 60 phase angle with helical distribution greater than 180 phase angle with normal distribution. Figure (15) shows the vector of velocity distribution in the wellbore and perforations. Also, comparison the inflow rate from perforation to wellbore between (60° phase angle with helical distribution and 180° phase angle with normal distribution).

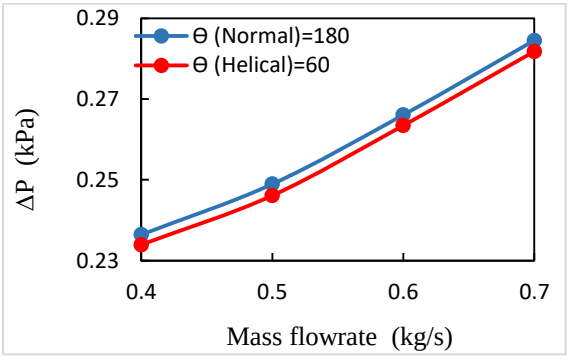

Fig. (11): Variation of pressure drop with inlet mass flowrate from porous media.

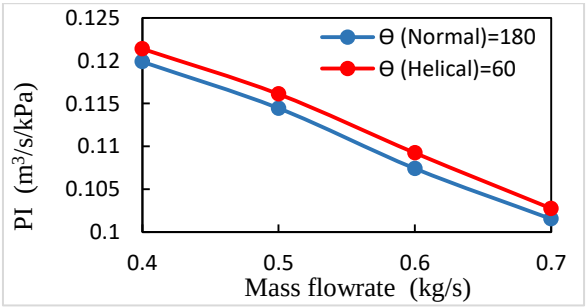

Fig. (12): Variation of productivity index with inlet mass flowrate from porous media

Open Access
No. 34 part 1, March 2022, pp. 85-104
P- ISSN: 2220-5381
E- ISSN: 2710-1096

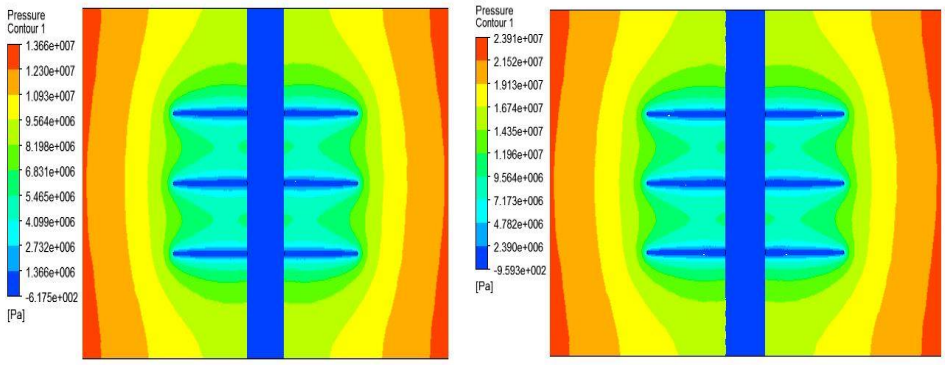

(a) 180° phase angle with $\dot{m} = 0.4$ kg/s (b) 180° phase angle with $\dot{m} = 0.7$ kg/s

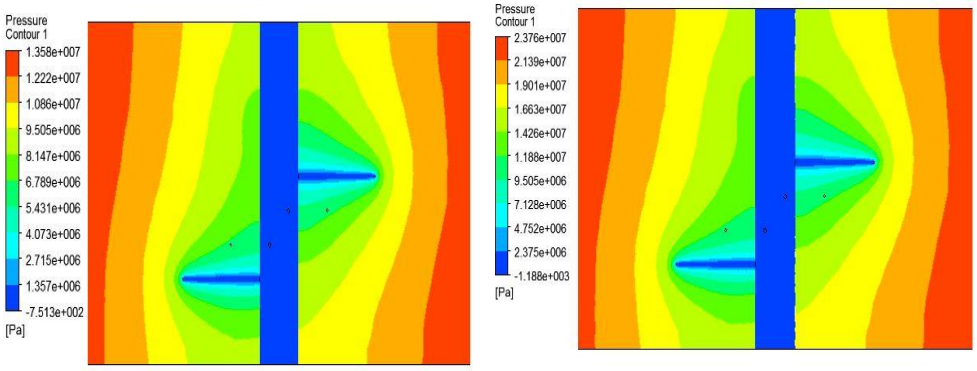

(c) 60° phase angle with $\dot{m} = 0.4$ kg/s (d) 60° phase angle with ṁ = 0.7 kg/s

Fig. (13): The pressure distribution contours with different of the phase angles and inlet mass flow rate from porous media.

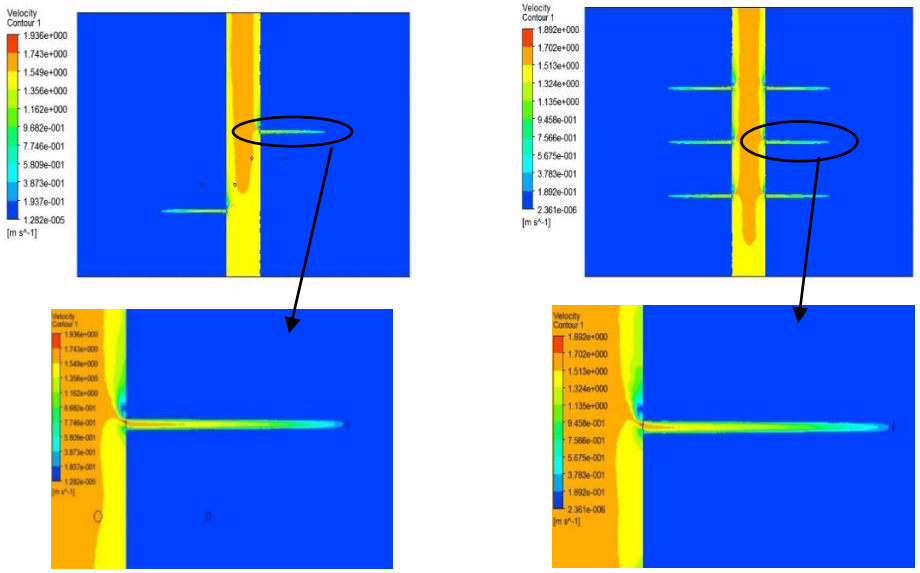

(a) 60° phase angle (b)180° phase angle

Fig. (14): The velocity contour with different of the phase angles and $\dot{m} = 0.7\ kg/s$ inlet mass flow rate from porous media.

Open Access
No. 34 part 1, March 2022, pp. 85-104
P- ISSN: 2220-5381
E- ISSN: 2710-1096

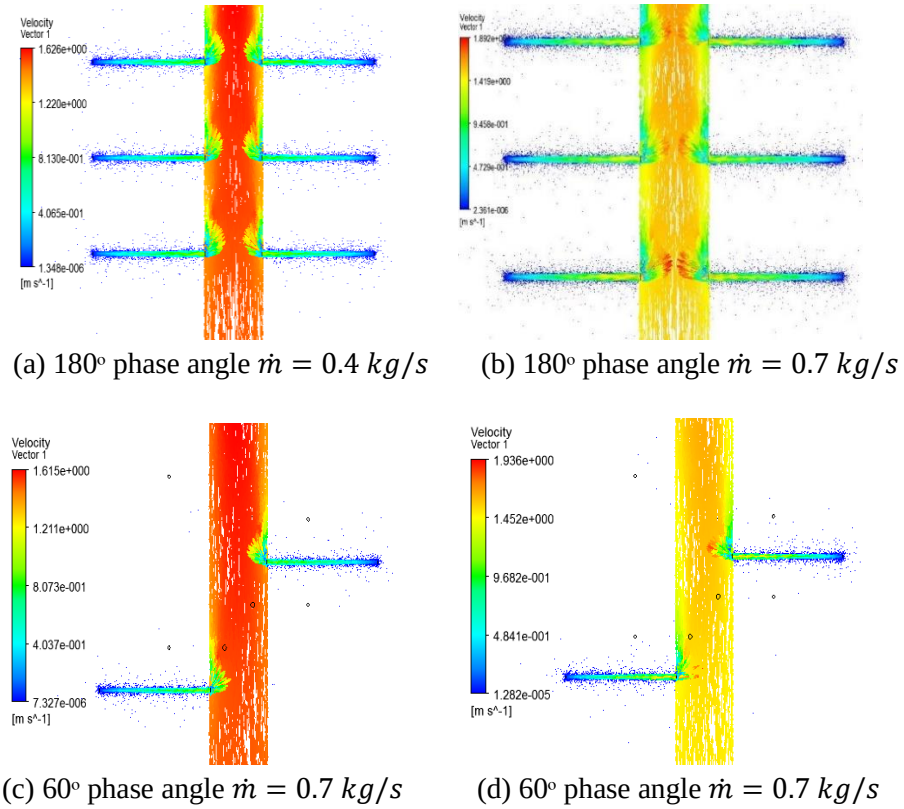

(a) 180° phase angle $\dot{m} = 0.4\ kg/s$ (b) 180° phase angle $\dot{m} = 0.7\ kg/s$

(c) 60° phase angle $\dot{m} = 0.7\ kg/s$ (d) 60° phase angle $\dot{m} = 0.7\ kg/s$

Fig. (15): Velocity vector for perforations of vertical wellbore with different inlet mass flow rate from porous media.

6.2 Effect of the Perforation Parameters

Figure (16) illustrates the variation of the pressure drop with perforation length, for four values of length which are (0.3, 0.35, 0.4, 0.45 m). The pressure drop increase with the increasing length of the perforations, due to increase interface area between perforations and porous media, this leads to increase inflow rate from perforation to wellbore. Also, the productivity index decreases with increasing length of the perforation, due to an increase of the pressure drop in the wellbore as shown in the Figure (17).

Figure (18) represents the contour of pressure distribution for the porous media surrounding the wellbore with different perforations length, for 60° phase angle with helical distribution and 180° phase angle with normal distribution. From the figure shows that, the pressure at the boundaries of the porous media decreases with increasing the perforations length, due to the increase of the flow area to the perforations.

Open Access
No. 34 part 1, March 2022, pp. 85-104
P- ISSN: 2220-5381
E- ISSN: 2710-1096

Figure (19) shows the velocity vector for the wellbore and perforations. Also, comparison of the flow rate from perforations to wellbore between (l_p= 0.30 and l_p=0.45 m) for 60° phase angle with helical distribution.

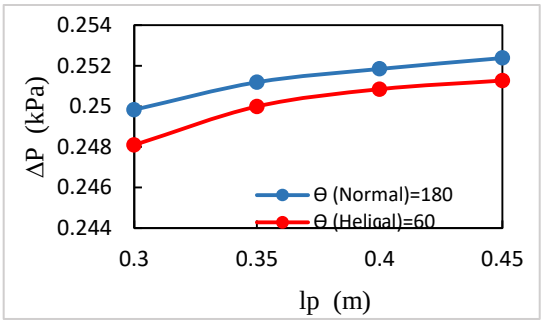

Fig. (16): Variation of the pressure drop with different length of perforations.

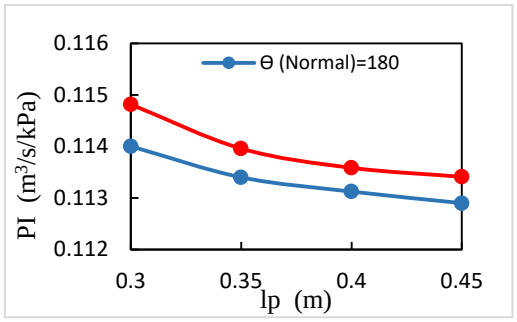

Fig. (17) Variation of the productivity index with different length of perforations.

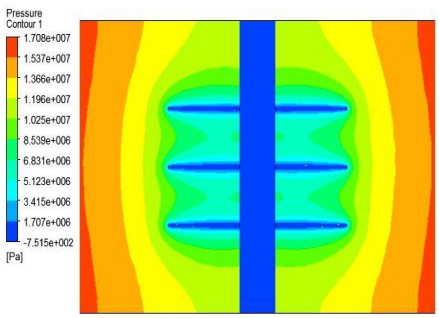

(a) 180° phase angle with l_p=0.30 m

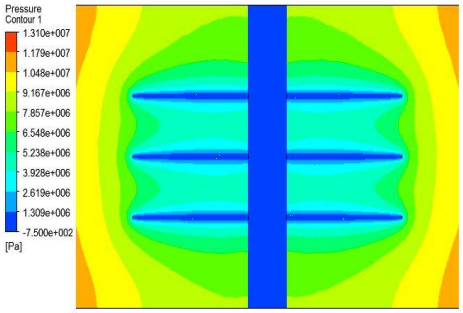

(b) 180° phase angle with l_p=0.45 m

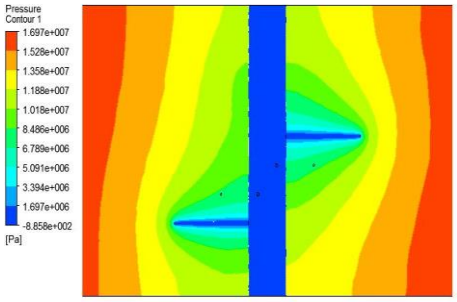

(c) 60° phase angle with l_p=0.30 m

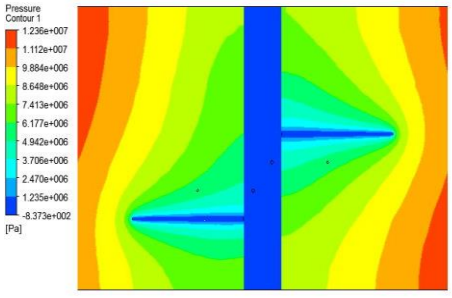

(d) 60° phase angle with l_p=0.45 m

Fig. (18): The pressure distribution contour with different of the phase angles and perforations diameter.

Open Access
No. 34 part 1, March 2022, pp. 85-104
P- ISSN: 2220-5381
E- ISSN: 2710-1096

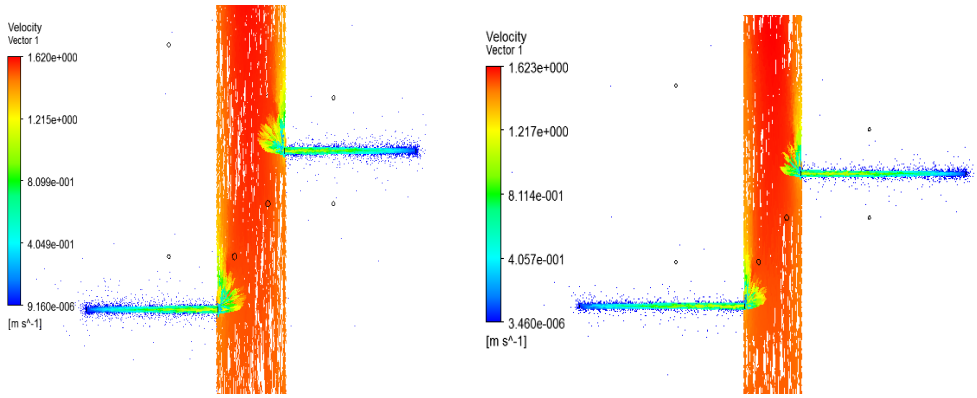

(a) 60° phase angle l_p=0.30 m (b) 60° phase angle l_p=0.45 m

Fig. (19): Velocity vector for a perforated vertical wellbore with different lengths of perforation.

Figure (20) demonstrate the variation of the pressure drop with different perforation diameters which are (8-13, 11-16, 14-19, 17-22 mm). The pressure drop increases with increasing the diameters of perforations, due to increase in the diameters leads to an increased inflow rate from perforations to the wellbore.

Figure (21) illustrates the variation of the productivity index with different perforation diameters. The productivity index decreases with increasing diameter of perforation due to the increase of pressure drop in the wellbore.

Figure (22) shows the pressure contour for the porous media surrounding the wellbore with (d_p=8-13 and d_p=17-22 mm), for 60° phase angle with helical distribution and 180° phase angle with normal distribution. Increasing the perforation diameter caused a significant variation of the pressure distribution in the porous media, due to the increased interface area between the perforations and the porous media.

Figure (23) shows the velocity vector for a perforated vertical wellbore for 180° phase angle with normal distribution. Also, comparison the inflow rate from perforations to wellbore between (dp=8-13 and dp=17-22 mm).

Open Access
No. 34 part 1, March 2022, pp. 85-104
P- ISSN: 2220-5381
E- ISSN: 2710-1096

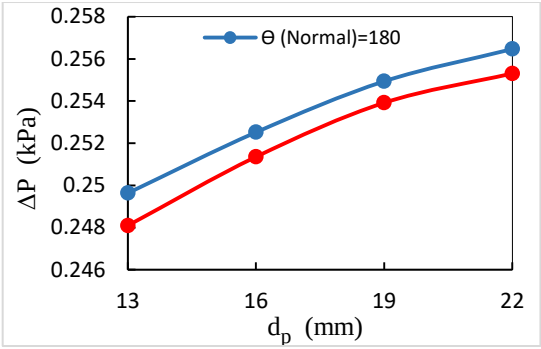

Fig. (20): Variation of the pressure drop with different perforations diameter.

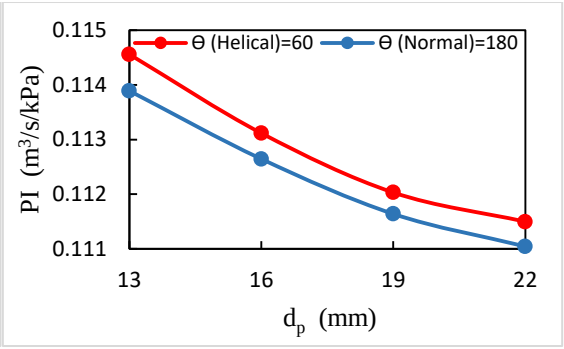

Fig. (21): Variation of productivity index with different diameter of perforations.

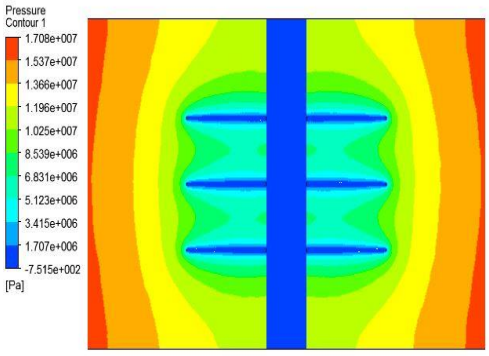

(a) 180° phase angle with d_p=13 mm

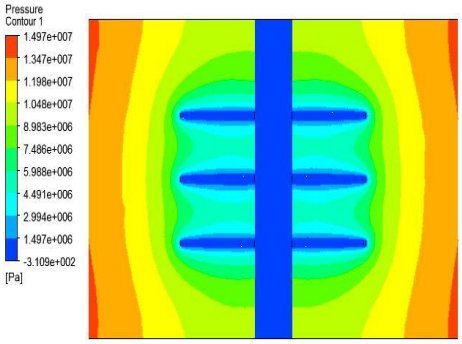

(b) 180° phase angle with d_p=22 mm

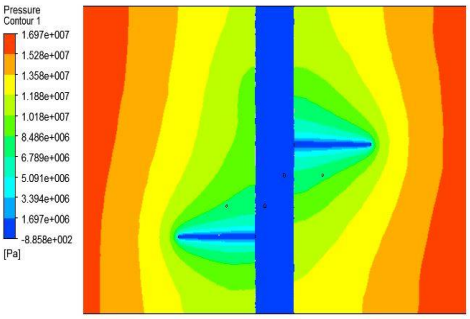

(c) 60° phase angle with d_p=13 mm

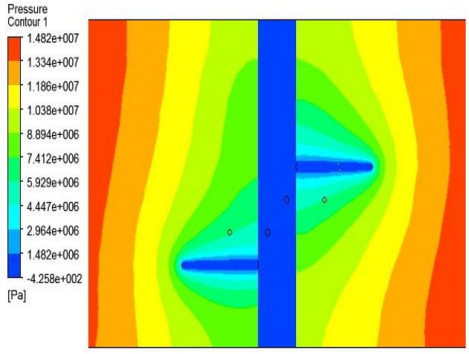

(d) 60° phase angle with d_p=22 mm

Fig. (22): The pressure distribution contour with different of the phase angles and perforations diameter.

Open Access
No. 34 part 1, March 2022, pp. 85-104
P- ISSN: 2220-5381
E- ISSN: 2710-1096

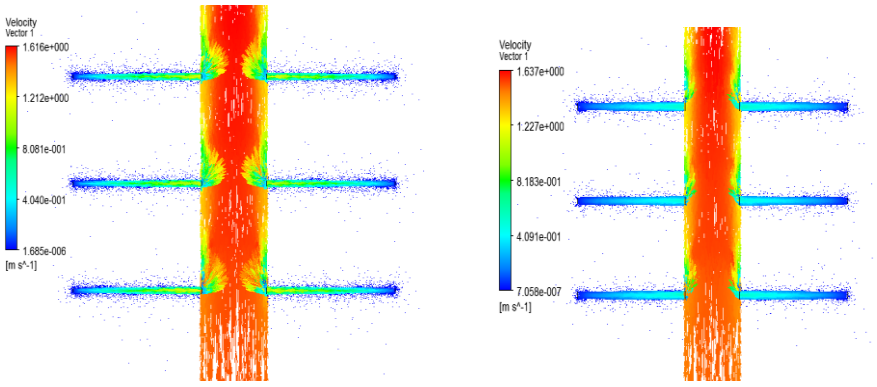

(a) 60° phase angle with d_p=8-13 mm. (b) 180° phase angle d_p=17-22 mm.

Fig. (23): Velocity vector for a perforation vertical wellbore.

7. Conclusion

The effect of pressure drop and productivity index on the performance of perforated vertical wellbores was studied. Also, the effect of the permeability of the zone surrounding the wellbore and parameters perforation. It was simulated by using CFD software. From the results obtained in this study, the following conclusions can be presented:

i. Increase the permeability of the porous media causing a decrease in the pressure drop. Also, productivity index increases with increasing the permeability of the porous media.

ii. The pressure drop increases with increasing inlet mass flow rate from porous media, while the productivity index decreasing.

iii. Increase of the perforations length has a few effects on the pressure drop and productivity index.

iv. Increase of the perforations diameter causing an increase in pressure drop. Also, the productivity index increases with increasing diameter of perforations.

v. In all cases, the 60° phase angle with helical distribution is better and has less losses than 180° phase angle with normal distribution.

Open Access
No. 34 part 1, March 2022, pp. 85-104
P- ISSN: 2220-5381
E- ISSN: 2710-1096

References

[1] Morris Muskat, "The Effect of Casing Perforations on Well Productivity," SPE. (1943); 151: 175-187.

[2] Stanley Locke,"An Advanced Method for Predicting the Productivity Ratio of a Perforated Well," SPE. 1981; 23(12): 2481-2488.

[3] M. Deo, S.M. Tariq, and P.M. Halleck,"Linear and Radial Flow Targets for Characterising Downhole Flow in Perforations," SPE. (1989); 4(3): 295-300.

[4] Metin Karakas and S.M. Tariq,"Semianalytical Productivity Models for Perforated Completions," SPE. 1991; 5: 73-82.

[5] Masaru Ihara, Koji Kikuyama and Keiichi Mizuguchi,"Flow in Horizontal Wellbores with Influx Through Porous Walls," SPE. 1994; 225-235.

[6] Y.S. Dogulu,"Modeling of Well Productivity in Perforated Completions," SPE-51048-MS, pp. 109-118, (1998).

[7] Yula Tang, Turhan Yildiz, Erdal Ozkan and Mohan G. Kelkar,"Effects of Formation Damage and High- Velocity Flow on the Productivity of Perforated Horizontal Wells,"SPE. 2005; 8: 315-324.

[8] Joseph Ansah, Mark A. Proett and Mohamed Y. Soliman. Advances in Well Completion Design: A New 3D Finite-Element Wellbore Inflow Model for Optimizing Performance of Perforated Completions. SPE. 2002; 1-11.

[9] E. Guerra and T. Yildiz, " A Simple Approximate Method to Predict Inflow Performance of Selectively Perforated Vertical Wells," SPE.2004.

[10] Turhan Yildiz. Assessment of Total Skin Factor in Perforated Wells. SPE. 2006; 9: 61-76.

[11] Jacques Hagoort," An analytical model for predicting the productivity of perforated wells," Journal of Petroleum Science and Engineering. 2007; 56: 199–218.

[12] Kuljabekov A.B., Inkarbekov M.K., Tungatarova M.S., Alibayeva K.A. and Kaltayev A , "Numerical Study of the Hydrodynamic Efficiency of the Multi-Stage Filter Setting Technology,"Archives of Mining Sciences. 2013; 58(3): 691-704.

Open Access
No. 34 part 1, March 2022, pp. 85-104
P- ISSN: 2220-5381
E- ISSN: 2710-1096

[13] Mahmoud O Elsharafi and Tibor Bodi,"Evaluation of the productivity of vertical oil wells by using different high shot density (HSD) guns," International Journal of Petrochemical Science & Engineering. 2017.

[14] Mohammed Abdulwahhab Abdulwahid, Sadoun Fahad Dakhil and I. N. Niranjan Kumar,"Numerical analysis of fluid flow properties in a partially perforated horizontal wellbore," American Journal of Energy Engineering. 2014; 2(6): 133-140.

[15] Thomas Vyzikas, "Application of numerical models and codes,"MERiFIC, 1st ed. (2014).

[16] Awbi H. B. ," Ventilation of Buildings," M.Sc. thesis, London, NewYork, Taylor, Francis, (2005).

[17] Harun Ates and M.G. Kelkar,"The Effect of Perforating on Oil Well Productivity," SPE. 1998; 2: 104-108.

[18] Mohammed K Salim1, Hussein S Sultan1 and Ahmed KM AL-Shara,"Effect of Shape and Parameters of Perforation in a Vertical Wellbore with Two Perforations (without Porous Media) on Pressure Drop,"Fluid Mechanics. 2017.